Anisotropic ferromagnetic polymer: A first step for their implementation in microfluidic systems

Damien Le Roy, Daya Dhungana, Laurence Ourry, Magalie Faivre, Rosaria Ferrigno, Alexandre Tamion, Véronique Dupuis, Vincent Salles, Anne-Laure Deman

Anisotropic ferromagnetic polymer: A first step for their implementation in microfluidic systems

Damien Le Roy, Daya Dhungana, Laurence Ourry, Magalie Faivre, Rosaria Ferrigno, Alexandre Tamion, Véronique Dupuis, Vincent Salles, and Anne-Laure Deman

Citation: AIP Advances **6**, 056604 (2016); doi: 10.1063/1.4943927
View online: http://dx.doi.org/10.1063/1.4943927
View Table of Contents: http://scitation.aip.org/content/aip/journal/adva/6/5?ver=pdfcov
Published by the AIP Publishing

Anisotropic ferromagnetic polymer: A first step for their implementation in microfluidic systems

Damien Le Roy,[1] Daya Dhungana,[2] Laurence Ourry,[2,3] Magalie Faivre,[2] Rosaria Ferrigno,[2] Alexandre Tamion,[1] Véronique Dupuis,[1] Vincent Salles,[3] and Anne-Laure Deman[2]

[1]*Institut Lumière Matière ILM-UMR 5306, CNRS, Université Lyon 1, Villeurbanne F-69622, France*

[2]*Institut des Nanotechnologies de Lyon INL-UMR5270, CNRS, Université Lyon 1, Villeurbanne F-69622, France*

[3]*Laboratoire Multimatériaux et Interfaces LMI-UMR 5615, CNRS, Université Lyon 1, Villeurbanne F-69622, France*

(Presented 14 January 2016; received 4 November 2015; accepted 31 December 2015; published online 9 March 2016)

Here we report on the influence of anisotropic microstructure on the performances of magnetically soft micro-patterns intended to integrate microfluidic systems. These micro-patterns are made of a composite obtained by mixing carbonyl iron particles with polydimethylsiloxane, which offers practical integration advantages. We investigated a wide range of magnetic particle loadings, from 10wt% to 83wt%, reaching magnetization as high as 630 kA/m. A homogeneous field was applied during the polymer's cross-linking phase so that to obtain a 1D arrangement of the particles in the solidified polymer, along the field direction. Here we present the results obtained for square-based micro-pillars prepared under a magnetic field applied along one of its diagonal. We assessed the magnetic anisotropy owing to the particles' spatial arrangement by comparing the magnetization processes along the two diagonals of the micro-pillar's base. The magnetic susceptibilities along the two directions differ from a factor greater than three. The results can be described in terms of high aspect ratio and porous magnetic agglomerates. [http://dx.doi.org/10.1063/1.4943927]

I. INTRODUCTION

Magnetic functions are powerful tools for microfluidic systems dedicated to biomedical applications.[1] In particular, *magnetophoresis*, which refers to the motion of an object in a magnetic field gradient, can be exploited in microsystems to perform concentration, separation or trapping functions of magnetically labeled cells,[2] deoxygenated red blood cells[3] or functionalized magnetic microbeads.[4] Three approaches have been so far developed to create magnetic field gradients at the micron scale: (1) micro-coils,[5] (2) micro-magnets[6–8] and (3) micro-concentrators of magnetic flux made of magnetically-soft materials.[9–11] In static conditions, Joule heating limits the performances of micro-coils, thus micro-magnets or micro-concentrators are generally preferred. Micro-magnets, permanently magnetized, are truly autonomous, but are limited to fixed force. In contrast micro-concentrators allow a remote control over the force intensity by varying the external field, so that to release trapped objects for subsequent analysis, or simply to pause sorting. For successful implementation of micro-concentrators in microfluidic channels, the magnetic material has to fulfill specific requirements. First, it must overcome technological bolts related to its heterogeneous integration with polymer, as most of the microfluidic systems are made of polymer, mainly PolyDiMethylSiloxane (PDMS). Second, it must be compatible with micro-patterning techniques and precisely localized inside or in the close region of the channel,[1,12] since accurate manipulation of micro-objects in microfluidic channels requires strong magnetic forces at the object's scale and over the entire channel height. As previously demonstrated magnetic PDMS composite is an elegant

approach to solve such technological issues.[9,13] Indeed, the composite preserves the properties of PDMS, such as soft-lithography 3D micro-structuration and O_2 surface activation for plasma bonding with glass and PDMS. In terms of desired magnetic properties, the micro-concentrators must combine high magnetization, no hysteretic reversal and high effective magnetic susceptibility. Recently, microfluidic devices integrating Carbonyl Iron/PDMS (I-PDMS) micro-patterns were realized and used to carry out the manipulation of paramagnetic beads and magnetically labeled cells,[9] showing competitive performances with metallic structures.

Micro-concentrators in general suffer from their relatively poor magnetic susceptibility. Indeed, once implemented in micro-channels, it is mainly the dimensions of the magnetic element, *via* its demagnetizing factors, that fix the apparent susceptibility, so the performances. In such open magnetic circuits, the high material's permeability often plays a minor role. Here we propose to explore a way to bypass this barrier using anisotropic composite. Several groups demonstrated the possibility of producing anisotropic composite polymer by organizing loaded magnetic particles in chains.[14,15] Likewise when it is exploited to reinforce mechanical[16,17] or electrical[18] properties of composite materials, it is proposed to use this principle to obtain high performance magnetic flux micro-concentrators.

In this paper, we report on the development of magnetically soft and anisotropic composite polymers, structured in square-based micro-pillars, with the aim of combining high magnetization and high susceptibility. The effect of 1D arrangement of the magnetic particles was studied over a wide range of concentrations. The composite microstructure was monitored by optical microscopy and related to magnetic characterization. We discuss the results in terms of anisotropic apparent susceptibility.

II. EXPERIMENTAL

A. Composite preparation

Carbonyl iron micro-particles (dry powder, 1-6μm diameter, 97% Fe basis) (Sigma-Aldrich) and PDMS mixture (10/1 w/w of monomer and curing agent, respectively) (Sylgard from Samaro) were thoroughly mixed in a mortar (around 4 min) until obtaining a homogeneous material prior to polymer reticulation. Different carbonyl iron concentrations of 10, 20, 30, 40, 50, 60, 70 and 83w% were tested.

B. Fabrication of I-PDMS micro-pillars

The molds were fabricated through standard photolithography method. Briefly, dry negative photoresist (Ethertec ®) was laminated on glass substrate in order to obtain 50 or 100 μm thick molds. I-PDMS was then plastered on the molds with a blade, taking care of cleaning any eventual smears on the surrounding photoresist with a tip. Microstructures identical to those integrated in micro-fluidic channels, i.e. 500 μm diagonal diamond shape, were realized for magnetic characterization. Pure PDMS was poured over the whole mold and heated (75°C for 60 min) to consecutively peel the composite micro-pillars off. Larger structures (squares, 5 mm in diagonal) were simultaneously realized for microscopic observations. For each concentration, two batches of samples were prepared in parallel: with and without applying a magnetic field, B_X, during the cross-linking step. In the following, the two series of samples are referred as S130 (B_X = 130 mT) and S0 (B_X = 0), respectively. The uniform field B_X of 130 mT, created in the gap between two permanent magnets, was applied for at least 12 hours at ambient temperature to let the particles move and form chains, prior to finalizing curing in an oven for two hours at 75°C. In contrast, S0 samples were directly cured at 75°C for two hours without being submitted to any magnetic field. Microfluidic devices integrating I-PDMS pillars, of S0 and S130 series, were realized following the previously reported experimental process.[9]

III. RESULTS AND DISCUSSION

Figure 1 shows in plane views of composite polymers, prepared as described in the previous section. In S0 samples (see Fig 1(b)), the carbonyl iron particles are found to be homogeneously

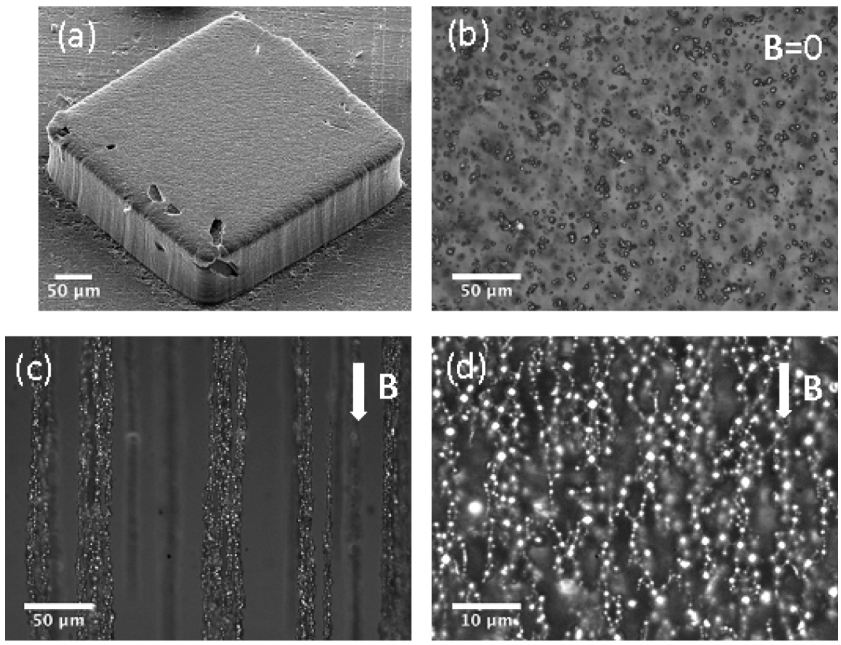

FIG. 1. (a) SEM image of a composite microstructure (500 µm diagonal diamond shape). Optical images of 10w% I-PDMS composites of S0 (b) and S130 (c) series, and 83w% I-PDMS of S130 (d).

dispersed within the PDMS matrix. Rapid cross-linking at 75°C enables to limit particles' sedimentation. This contrasts with the well-defined particle chains in low-concentration S130 samples (see Fig. 1(c)), where cross-linking was done at room temperature, and under a magnetic field. Magnetic dipolar interactions lead to the formation of 1D-shape agglomerates along the magnetic flux lines. The as-formed chains of particles are extended through the overall composite film dimension. One can observe clustering of chains, leading to a large distribution of agglomerate width, from the size of a single particle up to few tens of micrometers. At high concentration, one can observe large amount of ramifications between chains, though keeping an overall orientation along the field direction (see Fig. 1(d)).

The shape of the particle agglomerates is expected to induce magnetic anisotropy, as the demagnetizing field is reduced along the chain length. This could then increase the magnetic susceptibility along any desired direction, which is of great importance for use in microsystems. To bear this out, we carried out magnetic characterizations on our standard micro-pillar patterns, with a square base (see Fig. 1(a)), similar to the structures dedicated to be implemented in microfluidic channel. For each concentration, we systematically measured the magnetization curves along the two diagonals of the micro-pillar square base. The field applied during the cross-linking phase for the S130 samples was along one diagonal, hereinafter denoted as the X direction. As expected from the above-mentioned arguments about the chains' formation, the long axes of the agglomerates were systematically along X. Y refers to the direction of the second diagonal of the pillar's base, thus orthogonal to X. The square shape of the pillar implies that its "macroscopic" demagnetizing factors are the same along X and Y. That is expected for uniformly magnetized pillars, and that was what we measured on S0 samples, for which X and Y magnetization curves were found to superimpose.

Figure 2 shows the magnetization curves of 10wt% and 83wt% single pillars. The volume that is considered here is the entire volume of the pillar, be it for S0 or S130 samples. The obtained magnetization values are in good agreement with the expected values for a volume dilution of carbonyl iron particles (M_S of 1660 kA/m) into a non-magnetic matrix: 22 kA/m (10 wt%) and 631 kA/m (83 wt%). For the 83wt% sample, the magnetization is higher than the one of pure Ni (488 kA/m), and comparable with the ones of the benchmark soft magnetic metallic alloys such as Mumetal (517 kA/m), Supermalloy (637 kA/m) or Permalloy (850 kA/m). The volume

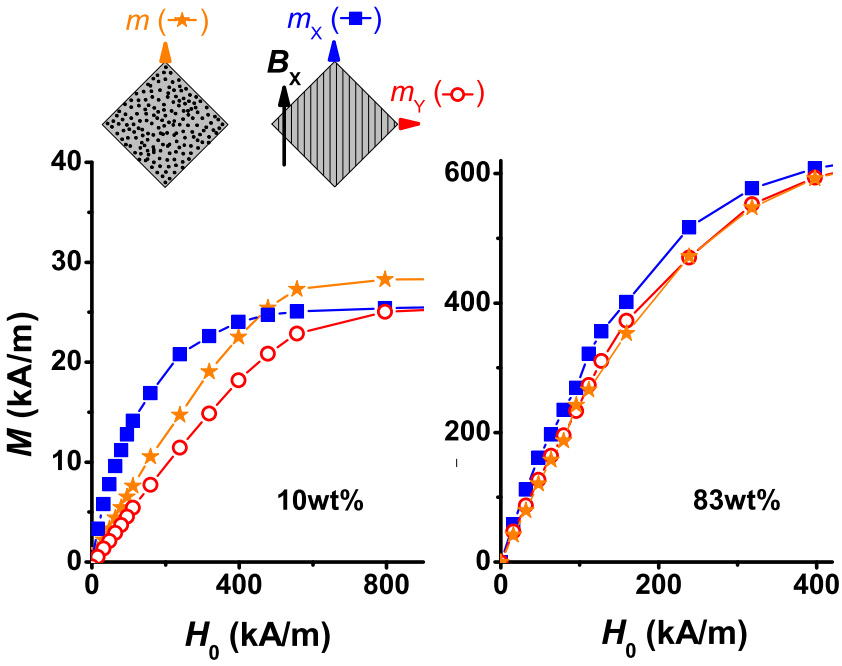

FIG. 2. Magnetization curves along the diagonal of homogeneously dispersed (stars, orange) and aligned (blue squares and red circles) particles, measured along *X* (squares) and *Y* (circles) directions, for two particle concentrations: (a) 10wt% and (b) 83wt%.

was estimated from contact profilometry analysis. The discrepancy of saturated magnetizations for the 10wt% samples, between the S0 and S130 samples, is attributed to the uncertainty in volume estimation. In the S130 samples, and through the overall concentration range, one can observe a difference of magnetization processes along *X* and *Y*, more pronounced at low concentration. The magnetization easy direction is systematically *X*, which supports that the origin of magnetic anisotropy is the particles' spatial 1D arrangement.

The figure of merit we used to assess the magnetic anisotropy is the ratio of the apparent susceptibility deduced from the reduced magnetization curves, χ_X/χ_Y (note that here the apparent susceptibility considered is the one of the reduced magnetization, thus expressed in m.kA^{-1}). The inset of Fig. 3 shows, as an example, χ_X and χ_Y on the magnetization curves of the 30wt% sample.

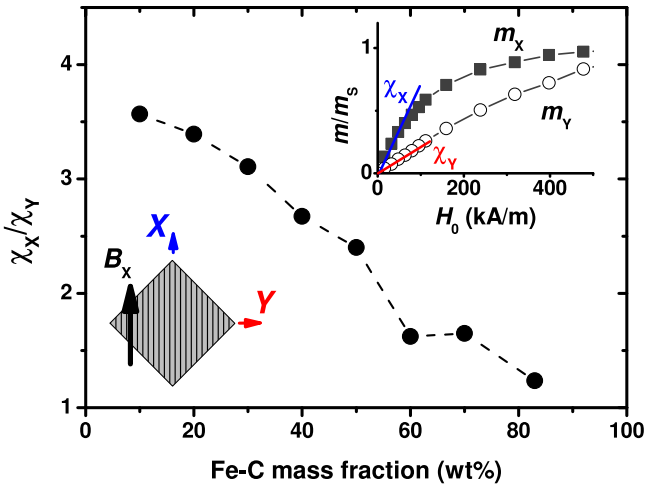

FIG. 3. Dependence of the pillars' magnetic anisotropy as a function of the Fe-C doping fraction. The inset shows how χ_X and χ_Y are determined from the reduced magnetization curves of a 30wt% composite pillar.

Fig. 3 displays the evolution of χ_X/χ_Y as a function of the composite's concentration, for similar pillars shape as the one of Fig. 1(a).

Considering an infinitely elongated rod along X, one can approximate the demagnetizing factor to the theoretical values $N_X = 0$ and $N_Y = N_Z = 1/2$. The magnetization is measured as a function of the applied field H_0, which differs from the internal field H by $H=H_0-NM$. Therefore, in the case of non-interacting chains, the susceptibility measured along X, noted χ_X, is the intrinsic magnetic susceptibility of the material χ_0. In contrast, along the Y direction, the magnetic susceptibility χ_Y is given by: $\chi_Y = \frac{\chi_0}{1+\frac{\chi_0}{2}}$. This leads to a ratio: $\frac{\chi_X}{\chi_Y} = 1 + \frac{\chi_0}{2}$. At low concentration, one can expect that the effect of dipolar interactions between adjacent chains would be minimum. In the 10wt% sample, we measured a X to Y susceptibility ratio of 3.6. It is several orders of magnitude below what could be calculated from intrinsic values of χ in ferromagnetic metals, but this can be expected for granular systems. From the obtained value of χ_X and the particles magnetization of 1660 kA/m, one expects χ_X/χ_Y to be of 6.4, still well above the measured value of 3.6. One can then estimate the correction to make on the value of the demagnetizing factor N_X (hereinbefore assumed to be 0) that this discrepancy would correspond to. Doing so, it comes $N_X = 0.06$ (resulting in: $\chi_X = \frac{\chi_0}{1+0.06\chi_0}$), so the one of an ellipsoid of revolution of major axes (a, a, c) with an aspect ratio c/a of around 5,[19] which is in contradiction to the microscopy observations (see Fig. 1(c)), even though the pillar edges delimit the aspect ratio range. Other sources of anisotropy reduction are thus to consider. Assuming the interactions are playing a minor role in the 10wt% sample (in which the inter-agglomerate distance is in average about 8 times their lateral size), one can allude to the effect of porosity in the particle agglomerates. In first approximation the impact of porosity can be seen as a reduction of the effective M_S of the 1D elements to consider. Our results can then be described by an average agglomerate compactness of 48%.

From our results, one cannot completely rule out interactions, even at low concentration. Indeed, χ_X/χ_Y is found to continuously decrease as the Fe-C fraction increases. This also suggests that the 1D organization is set at relatively low concentration, leading to sparse distribution of high aspect ratio agglomerates. The observed reduction of χ_X/χ_Y can be then attributed to the combined effect of (i) lateral chains growth and (ii) growing dipolar interactions between adjacent chains as their concentration increases. These dipolar interactions are demagnetizing along X and magnetizing along Y, thus fighting against the 1D-shape anisotropy.

Microfluidic devices integrating composite pillars were realized and their trapping efficiency of 12 μm superparamagnetic beads (SPB) (purchased from Kisker) was assessed. As a start, we selected the composite with 83wt% that presents the highest magnetization. Although the anisotropy revealed by the SQUID measurements is rather moderate, at the operating field of 143 kA/m, we measured a clear difference of magnetization: 325 kA/m for the S0 series (isotropic) and 378 kA/m along the X direction for the S130 series (anisotropic). This magnetization increase of 16% in the anisotropic pillar should contribute not only to an increase of the magnetic field and gradient at a given position in the channel but also to the capture length. Experimental results have shown that trapping efficiency was improved by a factor 2.2 at a flow rate of 500 μL/h using anisotropic composite pillars compared to isotropic composite pillars. In addition to the higher magnetization at the operating field, other mechanisms, hidden in the "macroscopic" magnetization measurements, may be involved. In particular, the periodic magnetization distribution owing to the formation of chain agglomerates in the anisotropic pillar may contribute to increase locally the magnetic field gradient in the close region of the pillar.

IV. CONCLUSION

In summary, composite polymers integrating high magnetization micro-particles were prepared, with concentration ranging from 10wt% to 83wt%. Applying a magnetic field during cross-linking is found to lead to high aspect ratio agglomerates of magnetic particles. We show that it is an efficient means to produce anisotropic magnetic composites, with inner high performance magnetic flux micro-concentrators. The anisotropy was investigated on composite micro-pillars, with suited dimensions to integrate microfluidic systems. The magnetism of such pillars was found

to be dominated by the inner 1D-shape anisotropy. Further development would involve to improve the compactness of agglomerates by studying the dynamic of their formation, the response to a larger applied field or the role of the magnetic particle shape. This enables to bypass the limitation set by the pillars' geometry, therefore demonstrating the great potential of composite polymer for the development of microfluidic systems.

ACKNOWLEDGEMENTS

The authors are indebted to the institute Carnot Ingénierie@Lyon for its support and funding. This work was also supported by the University of Lyon 1, through its program « BQR Accueil EC 2015 ». The authors are grateful to R. Checa for technical assistance at the « Centre de Magnétométrie de Lyon », and to J. Degouttes and N. Terrier for their technical support at the NanoLyon cleanroom facility.

[1] N. Pamme, Lab Chip **6**, 24-36 (2006).
[2] X. Yu, X. Feng, J. Hu, Z.-L. Zhang, and D.-W. Pang, Langmuir **27**, 5147 (2011).
[3] Y. Jung, Y. Choi, K.- H. Han, and A. B. Frazier, Biomed Microdev. **12**, 637-645 (2010).
[4] X. Yu, H.-S. Xia, Z.- D. Sun, K. Wang, J. Yu, H. Tang, D.-W. Pang, and Z.-L. Zhang, Biosensors and Bioelectronics. **41**, 129-136 (2013).
[5] R. Fulcrand, D. Jugieu, C. Escriba, A. Bancaud, D. Bourrier, A. Boukabache, and A. M. Gué, J. Micromech. Microeng. **19**, 105019 (2009).
[6] A. Walther, C. Marcoux, B. Desloges, R. Grechishkin, D. Givord, and N. M. Dempsey, J. Magn. Magn. Mater. **321**, 590-594 (2009).
[7] N. M. Dempsey, D. Le Roy, H. Marelli-Mathevon, G. Shaw, A. Dias, R. G. B. Framer, M. Khustov, L. F. Zanini, C. Villard, K. Hasselbach, C. Tomba, and F. Dumas-Bouchiat, Appl. Phys. Lett. **104**, 262401 (2014).
[8] F. Dumas-Bouchiat, L. F. Zanini, M. Kustov, N. M. Dempsey, R. Grechishkin, K. Hasselbach, J. C. Orlianges, C. Champeaux, A. Catherinot, and D. Givord, Appl. Phys. Lett. **96**, 102511 (2010).
[9] M. Faivre, R. Gelszinnis, J. Degouttes, N. Terrier, C. Rivière, R. Ferrigno, and A.-L. Deman, Biomicrofluidics **8**, 054103 (2014).
[10] P. Tseng, J. W. Judy, and D. Di Carlo, Nature Methods **9**(11), 1113-1119 (2012).
[11] T. Brunet, A. Bouclet, P. Ahmadi, D. Mitrossilis, B. Driquez, A.-C. Brunet, L. Henry, F. Serman, G. Béalle, C. Ménager, F. Dumas-Bouchiat, D. Givord, C. Yanicostas, D. Le Roy, N. M. Dempsey, A. Plessis, and E. Farge, Nature Communications **4**, 2821 (2013).
[12] Y.-J. Liu, S.-S. Guo, Z.-L. Zhang, W.-H. Huang, D. Baigl, M. Xie, Y. Chen, and D.-W. Pang, Electrophoresis **28**, 4713-4722 (2007).
[13] A.-L. Deman, M. Brun, M. Quatresous, J.-F. Chateaux, M. Frenea-Robin, N. Haddour, V. Semet, and R. Ferrigno, J. Micromech. Microeng. **21**, 095013 (2011).
[14] Y. Sahoo, M. Cheon, S. Wang, H. Luo, E. P. Furlani, and P.N. Prasad, J. Phys. Chem. B **108**, 3380-3383 (2004).
[15] D. Fragouli, R. Buonsanti, G. Bertoni, C. Sangregorio, C. Innocenti, A. Falqui, D. Gatteschi, P. D. Cozzoli, A. Athanassiou, and R. Cingolani, ACS Nano **4**, 1873-1878 (2010).
[16] R. L. Oréfice, L. L. Hench, and A. B. Brennan, J. Braz. Soc. Mech. Sci. **23** (2001).
[17] A. Ghosh and A. Verma, Fuel Cells **14**, 259-265 (2014).
[18] D. Fragouli, A. Das, C. Innocenti, Y. Guttikonda, S. Rahman, L. Liu, V. Caramia, C. M. Megaridis, and A. Athanassiou, ACS Appl. Mater. Interfaces **6**, 4535-4541 (2014).
[19] M. Bellegia, M. De Graff, and Y. Milev, Phil. Mag. **86**, 2451 (2006).